

A Bayesian Approach to Graphical Record Linkage and De-duplication

Rebecca C. Steorts¹, Rob Hall², and Stephen E. Fienberg¹

¹Department of Statistics, Carnegie Mellon University, Pittsburgh, PA 15213

²Etsy, Inc, Brooklyn, NY

{beka, fienberg } @ cmu.edu, rhall@etsy.com

March 2, 2022

Abstract

We propose an unsupervised approach for linking records across arbitrarily many files, while simultaneously detecting duplicate records within files. Our key innovation is to represent the pattern of links between records as a *bipartite* graph, in which records are directly linked to latent true individuals, and only indirectly linked to other records. This flexible new representation of the linkage structure naturally allows us to estimate the attributes of the unique observable people in the population, calculate transitive linkage probabilities across records (and represent this visually), and propagate the uncertainty of record linkage into later analyses. Our method makes it particularly easy to integrate record linkage with capture-recapture estimation. Our linkage structure lends itself to an efficient, linear-time, hybrid Markov chain Monte Carlo algorithm, which overcomes many obstacles encountered by previously proposed methods of record linkage, despite the high-dimensional parameter space. We illustrate our method using longitudinal data from the National Long Term Care Survey, where the tracking of individuals across waves let us objectively assess the accuracy of our record linkage.

1 Introduction

When data about individuals comes from multiple sources, it is essential to match, or link, records from different files that correspond to the same individual. Other names associated with record linkage are entity disambiguation and coreference resolution, meaning that records which are *linked* or *co-referent* can be thought of as corresponding to the same underlying *entity* (Christen, 2011). Solving this problem is not just important as a preliminary to statistical analysis; the noise and distortions in typical data files make it a difficult, and intrinsically high-dimensional, problem (Herzog, Scheuren and Winkler, 2007; Lahiri and Larsen, 2005; Winkler, 1999, 2000).

We propose a Bayesian approach to the record linkage problem based on a parametric model that addresses matching k files simultaneously and includes duplicate records within lists. We represent

29 the pattern of matches and non-matches as a bipartite graph, in which records are directly linked
30 to the true but latent individuals which they represent, and only indirectly linked to other records.
31 Such *linkage structures* allow us to simultaneously address three problems: record linkage, de-
32 duplication, and estimation of unique observable population attributes. The Bayesian paradigm
33 naturally handles uncertainty about linkage, which poses a difficult challenge to frequentist record
34 linkage techniques. (Liseo and Tancredi (2013) review Bayesian contributions to record linkage).
35 A Bayesian approach permits valid inference regarding posterior matching probabilities of records
36 and propagation of errors, as we discuss in Section 4.

37 To estimate our model, we develop a hybrid MCMC algorithm, in the spirit of Jain and Neal
38 (2004), which runs in linear time in the number of records and the number of MCMC iterations,
39 even in high-dimensional parameter spaces. Our algorithm permits duplication across and within
40 lists but runs faster if there are known to be no duplicates within lists. We achieve further gains
41 in speed using standard record linkage blocking techniques (Christen, 2011).

42 We apply our method to data from the National Long Term Care Survey (NLTC), which
43 tracked and surveyed approximately 20,000 people at five-year intervals. At each wave of the survey,
44 some individuals had died and were replaced by a new cohort, so the files contain overlapping but
45 not identical sets of individuals, with no within-file duplicates. We explore the validity of our
46 method using simulated data.

47 Section 2 provides a motivating example of the record linkage problem. In Section 3.1, we
48 introduce the notation and model, and describe the algorithm in Section 3.2. Sections 3.3 and 3.4
49 introduce posterior matching sets which upholding transitivity, and taking functions of the linkage
50 structure. In Sections 4 and 5 we apply the method to the the NLTC under two algorithms
51 (SMERE and SMERED). We evaluate each method compared to a simple baseline and explore the
52 validity of our method under simulation studies. We discuss future directions in Section 6.

53 1.1 Related Work

54 The classical work of Fellegi and Sunter (1969) considered linking two files in terms of Neyman-
55 Pearson hypothesis testing. Compared to this baseline, our approach is distinctive in that it

handles multiple files, models distortion explicitly, offers a Bayesian treatment of uncertainty and error propagation, and employs a sophisticated graphical data structure for inference to latent individuals. Methods based upon [Fellegi and Sunter \(1969\)](#) can extend to $k > 2$ files ([Sadinle and Fienberg, 2013](#)), but they break down for even moderately large k or complex data sets. Moreover, they provide little information about uncertainty in matches, or about the true values of noise-distorted records. [Copas and Hilton \(1990\)](#) describe the idea of modeling the distortion process using what they call the “Hit-Miss Model,” which anticipates part of our model in [Section 3.1](#). The specific distortion model we use is, however, closer to that introduced in [Hall and Fienberg \(2012\)](#), as part of a nonparametric frequentist technique for matching $k = 2$ files that allows for distorted data. Thus, their work is related to ours as we view the records as noisy, distorted entities, that we model using parameters and latent individuals.

Within the Bayesian paradigm, most work has focused on specialized approaches related to linking two files, which propagate uncertainty ([Belin and Rubin, 1995](#); [Gutman, Afendulis and Zaslavsky, 2013](#); [Larsen and Rubin, 2001](#); [Tancredi and Liseo, 2011](#)). These contributions, while valuable, do not easily generalize to multiple files and to duplicate detection.

Two recent papers ([Domingos and Domingos, 2004](#); [Gutman et al., 2013](#)) are most relevant to the novelty of our work, namely the linkage structure. To aid in the recovery of information about the population from distorted records, [Gutman et al. \(2013\)](#) called for developing “more sophisticated network data structures.” Our linkage graphs are one such data structure with the added benefit of permitting de-duplication and handling multiple files. Moreover, due to exact error propagation, we can easily integrate our methods with other analytic procedures. Algorithmically, the closest approach to our linkage structure is the graphical representation in [Domingos and Domingos \(2004\)](#), for de-duplication within one file. Their representation is a unipartite graph, where records are linked to each other. Our use of a bipartite graph with latent individuals naturally fits in the Bayesian paradigm along with distortion. Our method is the first to handle record linkage and de-duplication, while also modeling distortion and running in linear time.

82 2 Motivating Example

83 The databases (files) contain records regarding individuals that are distorted versions of their
84 unobserved true attributes (fields). We assume that each record corresponds to only one unobserved
85 latent individual. These distortions have various causes—measurement errors, transcription errors,
86 lies, etc.—which we do not model. We do, however, assume that the probability of distortion is the
87 same for all files (and we do so for computational convenience). Such distortions, and the lack of
88 unique identifiers shared across files, make it ambiguous when records refer to the same individuals.
89 This ambiguity can be reduced by increasing the amount of information available, either by adding
90 informative fields to each record, or, sometimes, by increasing the number of files.

91 We illustrate this issue with a motivating example of real world distortion and noise (see Table
92 1). With gender and state alone, these records could refer to (i) a single individual with a data
93 entry error (or old address, etc.) in one file; (ii) one individual correctly recorded as living in SC and
94 another correctly recorded in WV; (iii) two individuals with errors in at least one address; (iv) three
95 distinct individuals with correct addresses; (v) three individuals with errors in addresses. (There
96 are still further possibilities if the gender field might contain errors.) The goal is to determine
97 whether distinct records refer to the same individual, or to distinct individuals.

98 Table 1 illustrates a scenario where there is considerable uncertainty about whether two records
99 correspond to the same individual (under just gender and state). As we mentioned earlier, the
100 identities of the true individuals to which the records correspond are not entirely clear due to the
101 limited information available. Suppose we expand the field information by adding date of birth
102 (DOB) and race. We still have the same host of possibilities as before, but the addition of DOB
103 *may* let us make better decisions about matches. It is not clear if File 1 and File 2 are the same
104 person or different people (that just happen to have the same birthdate). However, the introduction
105 of DOB does make it more likely that File 3 is not the same person as in File 1 and File 2. The
106 method we propose in Section 3.1 deals with this type of noise; however, it proposes to deal with
107 noisier records in that they traditionally do not have identifying information such as name and
108 address, making the matching problem inherently difficult, even indeterminate.

	Gender	State	DOB	Race
File 1	F	SC	04/15/83	White
File 2	F	WV	04/15/83	White
File 3	F	SC	07/25/43	White

Table 1: Three files with year of birth and race.

3 Notation, Assumptions, and Linkage Structure

109

We begin by defining some notation, where we have k files or lists. For simplicity, we assume that all files contain the same p fields, which are all categorical, field ℓ having M_ℓ levels. We also assume that every record is complete. (Handling missing-at-random fields within records is a minor extension within the Bayesian framework (Reiter and Raghunathan, 2007).) Let \mathbf{x}_{ij} be the data for the j th record in file i , where $i = 1, \dots, k$, $j = 1, \dots, n_i$, and n_i is the number of records in file i ; \mathbf{x}_{ij} is a categorical vector of length p . Let $\mathbf{y}_{j'}$ be the latent vector of true field values for the j' th individual in the population (or rather aggregate sample), where $j' = 1, \dots, N$, N being the total number of *observed* individuals from the population. N could be as small as 1 if every record in every file refers to the same individual or as large as $N_{\max} \equiv \sum_{i=1}^k n_i$ if no datasets share any individuals.

110
111
112
113
114
115
116
117
118
119

Now define the linkage structure $\mathbf{\Lambda} = \{\lambda_{ij} ; i = 1, \dots, k ; j = 1, \dots, n_i\}$ where λ_{ij} is an integer from 1 to N_{\max} indicating which latent individual the j th record in file i refers to, i.e., \mathbf{x}_{ij} is a possibly-distorted measurement of $\mathbf{y}_{\lambda_{ij}}$. Finally, $z_{ij\ell}$ is 1 or 0 according to whether or not a particular field ℓ is distorted in \mathbf{x}_{ij} .

120
121
122
123

As usual, we use I for indicator functions (e.g., $I(x_{ij\ell} = m)$ is 1 when the ℓ th field in record j in file i has the value m), and δ_a for the distribution of a point mass at a (e.g., $\delta_{y_{\lambda_{ij}\ell}}$). The vector $\boldsymbol{\theta}_\ell$ of length M_ℓ denotes the multinomial probabilities. For clarity, we always index as follows: $i = 1, \dots, k; j = 1, \dots, n_i; j' = 1, \dots, N; \ell = 1, \dots, p; m = 1, \dots, M_\ell$. We provide an example of the linkage structure and a graphical representation in Appendix A.

124
125
126
127
128

129 **3.1 Independent Fields Model**

We assume that the files are conditionally independent, given the latent individuals, and that fields are independent within individuals (this is done for computational simplicity as is the motivation for our Bayesian model). We formulate the following Bayesian parametric model:

$$\begin{aligned}
 \mathbf{x}_{ij\ell} \mid \lambda_{ij}, \mathbf{y}_{\lambda_{ij\ell}}, z_{ij\ell}, \boldsymbol{\theta}_\ell &\stackrel{\text{ind}}{\sim} \begin{cases} \delta_{\mathbf{y}_{\lambda_{ij\ell}}} & \text{if } z_{ij\ell} = 0 \\ \text{MN}(1, \boldsymbol{\theta}_\ell) & \text{if } z_{ij\ell} = 1 \end{cases} \\
 z_{ij\ell} &\stackrel{\text{ind}}{\sim} \text{Bernoulli}(\beta_\ell) \\
 \mathbf{y}_{j'\ell} \mid \boldsymbol{\theta}_\ell &\stackrel{\text{ind}}{\sim} \text{MN}(1, \boldsymbol{\theta}_\ell) \\
 \boldsymbol{\theta}_\ell &\stackrel{\text{ind}}{\sim} \text{Dirichlet}(\boldsymbol{\mu}_\ell) \\
 \beta_\ell &\stackrel{\text{ind}}{\sim} \text{Beta}(a_\ell, b_\ell) \\
 \pi(\mathbf{\Lambda}) &\propto 1,
 \end{aligned}$$

130 where a_ℓ, b_ℓ , and $\boldsymbol{\mu}_\ell$ are all known.

131 **Remark 3.1:** We assume that every legal configuration of the λ_{ij} is equally likely a priori. This
 132 implies a non-uniform prior on related quantities, such as the number of individuals in the data.
 133 The uniform prior on $\mathbf{\Lambda}$ is convenient, since it simplifies computation of the posterior. Devising
 134 non-uniform priors over linkage structures remains a challenging problem both computationally
 135 and statistically, as sensible priors must remain invariant when permuting the labels of latent
 136 individuals, and cannot use covariate information about records.

Deriving the joint posterior and conditional distributions is mostly straightforward. One subtlety, however, is that \mathbf{y}, \mathbf{z} and $\mathbf{\Lambda}$ are all related, since if $z_{ij\ell} = 0$, then it must be the case that

$y_{\lambda_{ij\ell}} = x_{ij\ell}$. Taking this into account, the joint posterior is

$$\begin{aligned} \pi(\mathbf{\Lambda}, \mathbf{y}, \mathbf{z}, \boldsymbol{\theta}, \boldsymbol{\beta} \mid \mathbf{x}) &\propto \prod_{i,j,\ell,m} \left[(1 - z_{ij\ell}) \delta_{y_{\lambda_{ij\ell}}}(x_{ij\ell}) + z_{ij\ell} \theta_{\ell m}^{I(x_{ij\ell}=m)} \right] \\ &\times \prod_{\ell,m} \theta_{\ell m}^{\mu_{\ell m} + \sum_{j'=1}^N I(y_{j'\ell}=m)} \times \prod_{\ell} \beta_{\ell}^{a_{\ell}-1 + \sum_{i=1}^k \sum_{j=1}^{n_i} z_{ij\ell}} \\ &\times (1 - \beta_{\ell})^{b_{\ell}-1 + \sum_{i=1}^k \sum_{j=1}^{n_i} (1-z_{ij\ell})}. \end{aligned}$$

Now we consider the conditional distribution of \mathbf{y} . Here, the part of the posterior involving \mathbf{x} only matters for the conditional of \mathbf{y} when $z_{ij\ell} = 0$. Specifically, when $z_{ij\ell} = 0$, we know that $y_{\lambda_{ij\ell}} = x_{ij\ell}$. Next, for each $j' = 1, \dots, N$, let $R_{ij'} = \{j : \lambda_{ij} = j'\}$, so that \mathbf{x}_{ij} and $\mathbf{y}_{j'}$ refer to the same individual if and only if $j \in R_{ij'}$.

Remark 3.2: This notation allows the consideration of duplication within lists, i.e., distinct records within a list that correspond to the same individual. In particular, two records j_1 and j_2 in the same list i correspond to the same individual if and only if $\lambda_{ij_1} = \lambda_{ij_2}$. Implementing this in our hybrid MCMC is *simpler* than assuming the lists are already de-duplicated, since de-duplication implies that certain linkages are undefined.

From the joint posterior above, we can write down the full conditional distributions of $\boldsymbol{\theta}$ and $\boldsymbol{\beta}$ directly as

$$\beta_{\ell} \mid \mathbf{\Lambda}, \mathbf{z}, \boldsymbol{\theta}, \mathbf{y}, \mathbf{x} \sim \text{Beta} \left(a_{\ell} + \sum_{i=1}^k \sum_{j=1}^{n_i} z_{ij\ell}, b_{\ell} + \sum_{i=1}^k \sum_{j=1}^{n_i} (1 - z_{ij\ell}) \right)$$

for all ℓ and

$$\theta_{\ell m} \mid \mathbf{\Lambda}, \mathbf{z}, \mathbf{y}, \boldsymbol{\beta}, \mathbf{x} \sim \text{Dirichlet} \left(\mu_{\ell m} + \sum_{j'=1}^N y_{j'\ell} + \sum_{i=1}^k \sum_{j=1}^{n_i} z_{ij\ell} x_{ij\ell} + 1 \right),$$

for all ℓ and for each $m = 1, \dots, M_\ell$. Then

$$\mathbf{y}_{j'\ell} \mid \mathbf{\Lambda}, \mathbf{z}, \boldsymbol{\theta}, \boldsymbol{\beta}, \mathbf{x} \sim \begin{cases} \delta_{x_{ij\ell}} & \text{if there exist } i, j \in R_{ij'} \text{ such that } z_{ij\ell} = 0, \\ \text{Multinomial}(1, \boldsymbol{\theta}_\ell) & \text{otherwise.} \end{cases}$$

In other words, the linkage structure $\mathbf{\Lambda}$ tells us that $\mathbf{y}_{j'}$ corresponds to some \mathbf{x}_{ij} when there is no distortion. Now consider that \mathbf{z} represents the indicator of whether or not there is a distortion. When we condition on \mathbf{x}, \mathbf{y} , and $\mathbf{\Lambda}$, there are times when a distortion is certain. Specifically, if $x_{ij\ell} \neq y_{\lambda_{ij\ell}}$, then we know there must be a distortion, so $z_{ij\ell} = 1$. However, if $x_{ij\ell} = y_{\lambda_{ij\ell}}$, then $z_{ij\ell}$ may or may not equal 0. Therefore, we can show

$$\begin{aligned} & P(z_{ij\ell} = 1 \mid \mathbf{\Lambda}, \mathbf{y}, \boldsymbol{\theta}, \boldsymbol{\beta}, \mathbf{x}) \\ &= \frac{P(\mathbf{\Lambda}, \mathbf{y}, \boldsymbol{\theta}, \boldsymbol{\beta}, \mathbf{x} \mid z_{ij\ell} = 1)P(z_{ij\ell} = 1)}{P(\mathbf{\Lambda}, \mathbf{y}, \boldsymbol{\theta}, \boldsymbol{\beta}, \mathbf{x} \mid z_{ij\ell} = 1)P(z_{ij\ell} = 1) + P(\mathbf{\Lambda}, \mathbf{y}, \boldsymbol{\theta}, \boldsymbol{\beta}, \mathbf{x} \mid z_{ij\ell} = 0)P(z_{ij\ell} = 0)} \\ &= \frac{\beta_\ell \prod_{m=1}^{M_\ell} \theta_{\ell m}^{x_{ij\ell}}}{\beta_\ell \prod_{m=1}^{M_\ell} \theta_{\ell m}^{x_{ij\ell}} + (1 - \beta_\ell)}. \end{aligned}$$

Then we can write the conditional as

$$z_{ij\ell} \mid \mathbf{\Lambda}, \mathbf{y}, \boldsymbol{\theta}, \boldsymbol{\beta}, \mathbf{x} \stackrel{\text{ind}}{\sim} \text{Bernoulli}(p_{ij\ell}), \text{ where}$$

$$p_{ij\ell} = \begin{cases} 1 & \text{if } x_{ij\ell} \neq y_{\lambda_{ij\ell}} \\ \frac{\beta_\ell \prod_{m=1}^{M_\ell} \theta_{\ell m}^{x_{ij\ell}}}{\beta_\ell \prod_{m=1}^{M_\ell} \theta_{\ell m}^{x_{ij\ell}} + (1 - \beta_\ell)} & \text{if } x_{ij\ell} = y_{\lambda_{ij\ell}}, \end{cases} \quad \text{for all } \ell.$$

Finally, we derive the conditional distribution of $\mathbf{\Lambda}$. This is the only part of the model which changes if duplicates are allowed within lists. Conditional on \mathbf{x}, \mathbf{y} , and \mathbf{z} , there are many linkage structures that can be ruled out, i.e., that have probability zero. Specifically, for any i, j, ℓ such that $z_{ij\ell} = 0$, there is no distortion. This means that if $z_{ij\ell} = 0$, then for any c such that $x_{ij\ell} \neq y_{c\ell}$, we know that $\lambda_{ij} = c$ is impossible. On the other hand, if $z_{ij\ell} = 1$, then $\mathbf{x}_{ij\ell}$ simply comes from a multinomial, in which case the linkage structure is totally irrelevant. If we assume that no duplication is allowed within each list, then $j_1 \neq j_2$ implies that $\lambda_{ij_1} \neq \lambda_{ij_2}$. Additionally, we note

that for each file i , the part of the linkage structure corresponding to that dataset $(\lambda_{i1}, \dots, \lambda_{in_i})$ is independent of the linkage structures for the other datasets conditional on everything else. Then we can write the following (assuming no duplicates):

$$P(\lambda_{i1} = c_1, \dots, \lambda_{in_i} = c_{n_i} \mid \mathbf{y}, \mathbf{z}, \boldsymbol{\theta}, \boldsymbol{\beta}, \mathbf{x}) \stackrel{\text{ind}}{\propto} \begin{cases} 0 & \text{if there exist } j, \ell \text{ such that} \\ & z_{ij\ell} = 0 \text{ and } x_{ij\ell} \neq y_{c_j\ell}, \\ & \text{or if } c_{j_1} = c_{j_2} \text{ for any } j_1 \neq j_2 \\ 1 & \text{otherwise,} \end{cases}$$

where the somewhat nonstandard notation $\stackrel{\text{ind}}{\propto}$ simply denotes that distributions for different i are independent. 146
147

Allowing duplicates within lists, we find that the conditional distribution lifts a restriction from the one just derived. That is,

$$P(\lambda_{i1} = c_1, \dots, \lambda_{in_i} = c_{n_i} \mid \mathbf{y}, \mathbf{z}, \boldsymbol{\theta}, \boldsymbol{\beta}, \mathbf{x}) \stackrel{\text{ind}}{\propto} \begin{cases} 0 & \text{if there exist } j, \ell \text{ such that} \\ & z_{ij\ell} = 0 \text{ and } x_{ij\ell} \neq y_{c_j\ell}, \\ 1 & \text{otherwise.} \end{cases}$$

3.2 Split and MERge REcord linkage and De-duplication (SMERED) Algorithm 148

Our main goal is estimating the posterior distribution of the linkage (i.e., the clustering of records into latent individuals). The simplest way of accomplishing this is via Gibbs sampling. We could iterate through the records, and for each record, sample a new assignment to an individual (from among the individuals represented in the remaining records, plus an individual comprising only that record). However, this requires the quadratic-time checking of proposed linkages for every record. Thus, instead of Gibbs sampling, we use a hybrid MCMC algorithm to explore the space of possible linkage structures, which allows our algorithm to run in linear time. 149
150
151
152
153
154
155

Our hybrid MCMC takes advantage of split-merge moves, as done in [Jain and Neal \(2004\)](#), which avoids the problems associated with Gibbs sampling, even though the number of parameters 156
157

158 grows with the number of records. This is accomplished via proposals that can traverse the state
159 space quickly and frequently visit high-probability modes, since the algorithm splits or merges
160 records in each update, and hence, frequent updates of the Gibbs sampler are not necessary.

161 Furthermore, a common technique in record linkage is to require an exact match in certain
162 fields (e.g., birth year) if records are to be linked. This technique of *blocking* can greatly reduce
163 the number of possible links between records (see, e.g., [Winkler, 2000](#)). Since blocking gives up on
164 finding truly co-referent records which disagree on those fields, it is best to block on fields that have
165 little or no distortion. We block on the fairly reliable fields of sex and birth year in our application
166 to the NLTCs below. A strength of our model is that it incorporates blocking organically. Setting
167 $b_\ell = \infty$ for a particular field ℓ forces the distortion probability for that field to zero. This requires
168 matching records to agree on the ℓ th field, just like blocking.

169 We now discuss how the split-merge process links records to records, which it does by assigning
170 records to latent individuals. Instead of sampling assignments at the record level, we do so at the
171 individual level. Initially, each record is assigned to a unique individual. On each iteration, we
172 choose two records at random. If the pair belong to *distinct* latent individuals, then we propose
173 merging those individuals to form a single new latent individual (i.e., we propose that those records
174 are co-referent). On the other hand, if the two records belong to the *same* latent individual, then
175 we propose splitting it into two new latent individuals, each seeded with one of the two chosen
176 records, and the other records randomly divided between the two. Proposed splits and merges are
177 accepted based on the Metropolis-Hastings ratio and rejected otherwise.

178 Sampling from all possible pairs of records will sometimes lead to proposals to merge records
179 in the same list. If we permit duplication within lists, then this is not a problem. However, if we
180 know (or assume) there are no duplicates within lists, we should avoid wasting time on such pairs.
181 The no-duplication version of our algorithm does precisely this. (See [Appendix B](#) for the algorithm
182 and pseudocode.) When there are no duplicates within files, we call this the SMERE (Split and
183 MErge REcord linkage) algorithm, which enforces the restriction that $R_{ij'}$ must be either \emptyset or a
184 single record. This is done through limiting the proposal of record pairs to those in distinct files;
185 the algorithm otherwise matches SMERED.

3.3 Posterior Matching Sets and Linkage Probabilities

186

In a Bayesian framework, the output of record linkage is not a deterministic set of matches between records, but a probabilistic description of how likely records are to be co-referent, based on the observed data. Since we are linking multiple files at once, we propose a range of posterior matching probabilities: the posterior probability of linkage between two arbitrary records and more generally among k records, the posterior probability that a given set of records is linked, and the posterior probability that a given set of records is a maximal matching set (which will be defined later).

Two records (i_1, j_1) and (i_2, j_2) *match* if they point to the same latent individual, i.e., if $\lambda_{i_1 j_1} = \lambda_{i_2 j_2}$. The posterior probability of a match can be computed from the S_G MCMC samples:

$$P(\lambda_{i_1 j_1} = \lambda_{i_2 j_2} | \mathbf{X}) = \frac{1}{S_G} \sum_{h=1}^{S_G} I(\lambda_{i_1 j_1}^{(h)} = \lambda_{i_2 j_2}^{(h)}).$$

A one-way match occurs when an individual appears in only one of the k files, while a two-way match is when an individual appears in exactly two of the k files, and so on (up to k -way matches). We approximate the posterior probability of arbitrary one-way, two-way, \dots , k -way matches as the ratio of frequency of those matches in the posterior sample to S_G .

Although probabilistic results and interpretations provided by the Bayesian paradigm are useful both quantitatively and conceptually, we often need to report a point estimate of the linkage structure. Thus, we face the question of how to condense the overall posterior distribution of $\mathbf{\Lambda}$ into a single estimated linkage structure.

Perhaps the most obvious approach is to set some threshold v , where $0 < v < 1$, and to declare (i.e., estimate) that two records match if and only if their posterior matching probability exceeds v . This strategy is useful if only a few specific pairs of records are of interest, but its flaws are exposed when we consider the coherence of the overall estimated linkage structure implied by such a thresholding strategy. Note that the true linkage structure is *transitive* in the following sense: if records A and B are the same individual, and records B and C are the same individual, then records A and C must be the same individual as well. This requirement of transitivity, however, is in no way enforced by the simple thresholding strategy described above. Thus, a more sophisticated approach

209 is required if the goal is to produce an estimated linkage structure that preserves transitivity.

To this end, it is useful to define a new concept. A set of records \mathcal{A} is a *maximal matching set* (MMS) if every record in the set has the same value of λ_{ij} and no record outside the set has that value of λ_{ij} . Define $\Omega(\mathcal{A}, \mathbf{\Lambda})$ to be 1 if \mathcal{A} is an MMS in $\mathbf{\Lambda}$ and 0 otherwise:

$$\Omega(\mathcal{A}, \mathbf{\Lambda}) = \sum_{j'} \left(\prod_{(i,j) \in \mathcal{A}} I(\lambda_{ij} = j') \prod_{(i,j) \notin \mathcal{A}} I(\lambda_{ij} \neq j') \right).$$

Essentially, records are in the same maximal matching set if and only if they match the same latent individual, though which individual is irrelevant. Given a set of records \mathcal{A} , the posterior probability that it is an MMS in $\mathbf{\Lambda}$ is simply

$$P(\Omega(\mathcal{A}, \mathbf{\Lambda}) = 1) = \frac{1}{S_G} \sum_{h=1}^{S_G} \Omega(\mathcal{A}, \mathbf{\Lambda}^{(h)}).$$

210 The MMSs allow a more sophisticated method of preserving transitivity when estimating a single
 211 overall linkage structure. For any record (i, j) , its *most probable MMS* \mathcal{M}_{ij} is the set containing (i, j)
 212 with the highest posterior probability of being an MMS, i.e., $\mathcal{M}_{ij} := \arg \max_{\mathcal{A}: (i,j) \in \mathcal{A}} P(\Omega(\mathcal{A}, \mathbf{\Lambda}) =$
 213 $1)$. Note, however, that there are still problems with a strategy of linking each record to exactly
 214 those other records in its most probable maximal matching set. Specifically, it is possible for
 215 different records' most probable maximal matching sets to contradict each other. For example,
 216 Record A may be in Record B's most probable maximal matching set, but Record B may not be
 217 in Record A's most probable maximal matching set. To solve this problem, we define a *shared*
 218 *most probable MMS* to be a set that is the most probable MMS for each of its members. We then
 219 estimate the overall linkage structure by linking records if and only if they are in the same shared
 220 most probable MMS. The resulting linkage structure is by construction transitive. We illustrate
 221 examples of MMSs and shared most probable MMSs in Section 4.2.

3.4 Functions of Linkage Structure

222

The output of the Gibbs sampler also allows us to estimate the value of any function of the variables, parameters, and linkage structure by computing the average value of the function over the posterior samples. For example, estimated summary statistics about the population of latent individuals are straightforward to calculate. Indeed, the ease with which such estimates can be obtained is yet another benefit of the Bayesian paradigm, and of MCMC in particular.

223

224

225

226

227

4 Assessing Accuracy of Matching and Application to NLTCs

228

We test our model using data from the National Long Term Care Survey (NLTCs), a longitudinal study of the health of elderly (65+) individuals (<http://www.nltcs.aas.duke.edu/>). The NLTCs was conducted approximately every six years, with each wave containing roughly 20,000 individuals. Two aspects of the NLTCs make it suitable for our purposes: individuals were tracked from wave to wave with unique identifiers, but at each wave, many patients had died (or otherwise left the study) and were replaced by newly-eligible patients. We can test the ability of our model to link records across files by seeing how well it is able to track individuals across waves, and compare its estimates to the ground truth provided by the unique identifiers.

229

230

231

232

233

234

235

236

To show how little information our method needs to find links across files, we gave it access to only four variables, all known to be noisy: date of birth, sex, state of residence, and the regional office at which the subject was interviewed. We linked individuals across the 1982, 1989, and 1994 survey waves. Our model had little information on which to link, and not *all* of its assumptions strictly hold (e.g., individuals can move between states across waves). We demonstrate our method's validity using error rates, confusion matrices, posterior matching sets and linkage probabilities, and estimation of the unknown number of observed individuals from the population.

237

238

239

240

241

242

243

Appendix C provides a simulation study of the NLTCs with varying levels of distortion at the field level. We conclude from this that SMERE is able to handle low to moderate levels of distortion (Figure 8). Furthermore, as distortion increases, so do the false negative rate (FNR) and false positive rate (FPR) (Figure 7).

244

245

246

247

248 4.1 Error Rates and Confusion Matrix

249 Since we have unique identifiers for the NLTCs, we can see how accurately our model matches
250 records. A *true link* is a match between records which really do refer to the same latent individual;
251 a *false link* is a match between records which refer to different latent individuals; and a *missing*
252 *link* is a match which is not found by the model. Table 5 gives posterior means for the number of
253 true, false, and missing links. For the NLTCs, the FNR is 0.11, while the FPR is 0.046, when we
254 block by date of birth year (DOB) and sex.

255 More refined information about linkage errors comes from a confusion matrix, which compares
256 records' estimated and actual linkage patterns (Figure 1 and Table 6 in Appendix D). Every row
257 in the confusion matrix is diagonally dominated, indicating that correct classifications are over-
258 whelmingly probable. The largest off-diagonal entry, indicating a mis-classification, is 0.07. For
259 instance, if a record is estimated to be in both the 1982 and 1989 waves, it is 90% probable that this
260 estimate is correct. If the true pattern for 1982 and 1989 is wrong, the estimate is most probably
261 1982 (0.043) and 1989 (0.033) followed by all years (0.018), and then the other waves with
262 small estimated probabilities.

263 4.2 Example of Posterior Matching Probabilities

264 We wish to search for sets of records that match record 10084 in 1982. In the posterior samples
265 of $\mathbf{\Lambda}$, this record is part of three maximal matching sets that occur with nonzero estimated posterior
266 probability, one with high and two with low posterior matching probabilities (Table 3). This record
267 has a posterior probability of 0.995 of simultaneously matching both record 6131 in 1989 and record
268 5583 in 1994. All three records denote a male, born 07/01/1910, visiting office 25 and residing in
269 state 14. The unique identifiers show that these three records are in fact the same individual.
270 Practically speaking, only matching sets with reasonably large posterior probability, such as the
271 set in the last column of Table 3, are of interest.

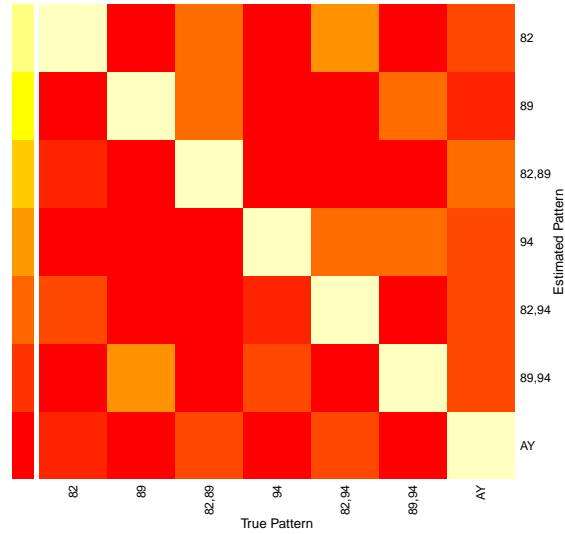


Figure 1: Heatmap of relative probabilities from the confusion matrix, running from yellow (most probable) to dark red (probability 0). The largest probabilities are on the diagonal, showing that the linkage patterns estimated for records are correct with high probability. Mis-classification rates are low and show a tendency to under-link rather than over-link.

4.3 Example of Most Probable MMSs

272

For each record in the NLTCS, we wish to produce its most probable maximal matching set (MP- 273
MMS). We then wish to identify those MPMMSs that are shared MPMMSs. Finally, we wish to 274
show the linked records for the shared most probable MMSs visually for a subset of the NLTCS (it 275
is too large to show for the entire dataset). 276

On each Gibbs iteration, we record all the records linked to a given latent individual; this is an 277
MMS. We aggregate MMSs across Gibbs iterations, and their relative frequencies are approximate 278
posterior probabilities for each MMS. Each record is labeled with the most probable MMS to which 279
it belongs. Finally, we link two records when they share the same most probable MMS, giving us 280
the shared most probable MMS. From this we are able to compute a FNR and a FPR (which we 281
discuss in Section 5.1). We give an example of the most probable MMSs for the first ten rows in 282
Table 2. 283

In Figure 2, we provide the shared most probable MMSs for the first 204 records of the NLTCS. 284
Color indicates whether or not the probability of a shared most probable MMS was above (green) 285

record	MPMMS	posterior probability
1.0	{1.0, 1.16651}	0.51
1.16651	{1.0, 1.16651}	0.51
1.1	{1.1}	1.00
1.10	{1.10}	0.75
1.2024	{1.2024, 1.21667, 1.39026}	0.82
1.3043	{1.3043}	0.58
1.21667	{1.2024, 1.21667, 1.39026}	0.82
1.39026	{1.2024, 1.21667, 1.39026}	0.82
1.2105	{1.2105, 1.21719, 1.39079}	0.81
1.21719	{1.2105, 1.21719, 1.39079}	0.81

Table 2: First 10 rows of most probable maximal matching sets.

286 or below (red) the value 0.8. Transitivity is clear from the fact that each connected component is
287 a clique, i.e., each record is connected to every other record in the same set. In Figure 3, we replot
288 the same records, however, we add a feature to each set. Each edge is either straight or curvy
289 to indicate whether the link was correct (straight) or incorrect (curvy) according to the ground
290 truth from the NLTCs. Overall, we see that the the curvy sets tend to be red, meaning that these
291 matches were assigned a lower posterior probability by the model, while the straight sets tend to
292 be green, meaning that these matches were assigned a higher posterior probability by the model.

293 We can view the red wavy links as individuals we would push to clerical review since the
294 algorithms has trouble matching them. For the NLTCs, manual review would possibly not do
295 much better than our algorithm since there many individuals match on everything except unique
296 ID. Since there is no other information to match on, we cannot hope to improve in this application.

297 Useful as these figures are, they would become visually unreadable for the *entire* NLTCs or
298 any record linkage problem of this scale or larger. This is a first step at showing that shared
299 most probable MMSs can be visualized. Visualization on the entire graph structure would be an
300 important advancement moving forward.

301 4.4 Estimation of Attributes of Observed Individuals from the Population

302 The number of observed unique individuals N is easily inferred from the posterior of $\mathbf{\Lambda}|\mathbf{X}$, since
303 N is simply the number of unique values in $\mathbf{\Lambda}$. Defining $N|\mathbf{X}$ to be the posterior distribution

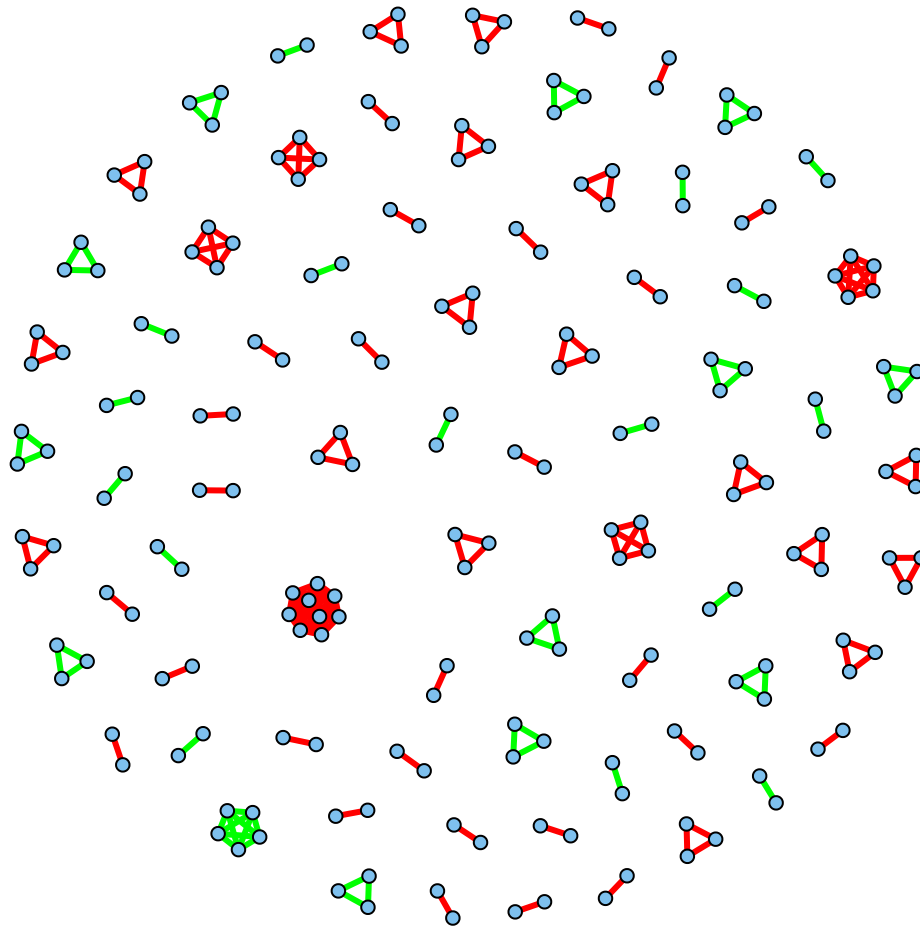


Figure 2: This illustrates the first 204 records, where each node is a record and edges are drawn between records with shared most probable MMSs. Transitivity is clear from the fact that each connected component is a clique, or rather, each record is connected to every other record in the same set. Color indicates whether or not the probability of the shared most probable MMS was above (green) or below (red) a threshold of 0.8.

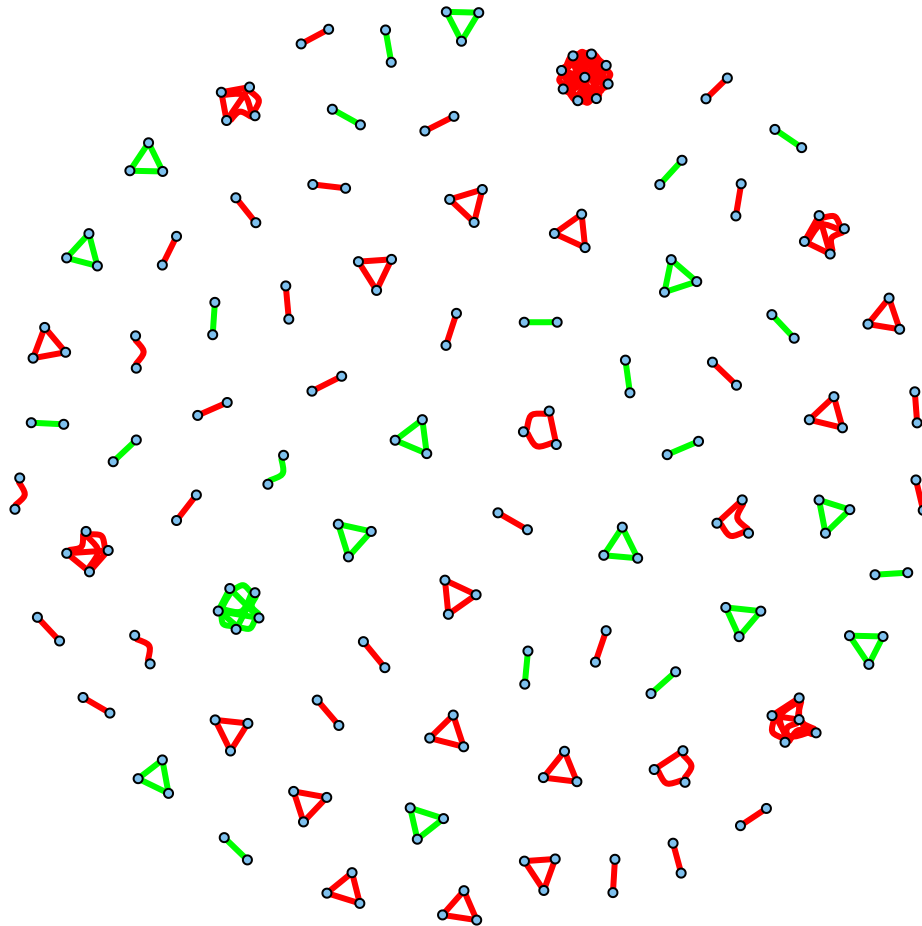


Figure 3: The same as Figure 2 with two added features: there are curvy and straight edges. The curvy edges indicate that SMERED and the NLTCS do not agree on the linkage, hence a false link. The straight edges indicate linkage agreement. We can see that there are a fair number of red, wavy edges indicating low probability and incorrect links. There are also many straight edged green high probability correct links. This illustrates one level of accuracy of the algorithm in the sense that it finds correct links and identifies incorrect ones. We can view the red links as individuals we would push to clerical review since the algorithms has trouble matching them (if this is warranted).

of N , we can find this by applying a function to the posterior distribution on \mathbf{A} , as discussed in 304
 Section 3.4. (Specifically, $N = |\#\mathbf{A}|$, where $\#\mathbf{A}$ maps \mathbf{A} to its set of unique entries, and $|A|$ is the 305
 cardinality of the set A .) Doing so, the posterior distribution of $N|\mathbf{X}$ is given in Figure 4. Also, 306
 $\hat{N} := E(N|\mathbf{X}) = 35,992$ with a posterior standard error of 19.08. Since the true number of observed 307
 unique individuals is 34,945, we are slightly undermatching, which leads to an overestimate of N . 308
 This phenomenon most likely occurs due to patients migrating between states across the three 309
 different waves. It is difficult to improve this estimate since we do not have additional information 310
 as described above. 311

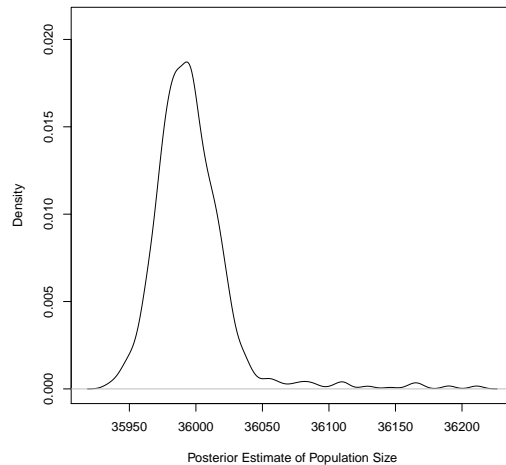


Figure 4: Posterior density of the number of observed unique individuals N .

We can also estimate attributes of sub-groups. For example, we can estimate the number of individuals within each wave or combination of waves—that is, the number of individuals with any given linkage pattern. (We summarize these estimates here with posterior expectations alone, but the full posterior distributions are easily computed.) Recall for each $j' = 1, \dots, N$, $R_{ij'} = \{j : \lambda_{ij} = j'\}$. For example, the posterior expectation for the number of individuals appearing in lists i_1 and i_2 but not i_3 is approximately

$$\frac{1}{S_G} \sum_{h=1}^{S_G} \sum_{j'} I(|R_{i_1 j'}^{(h)}| = 1) I(|R_{i_2 j'}^{(h)}| = 1) I(|R_{i_3 j'}^{(h)}| = 0).$$

312 (The inner sum is a function of $\mathbf{A}^{(h)}$, but a complicated one to express without the R_{ij} .)

313 Table 4 reports the posterior means for the overlapping waves and each single wave of the
314 NLTCs and compares this to the ground truth. In the first wave (1982), our estimates perform
315 exceedingly well with relative error of 0.11%, however, as waves cross and we try to match people
316 based on limited information, the relative errors range from 8% to 15%. This is not surprising,
317 since as patients age, we expect their proxies to respond, making patient data more prone to errors.
318 Also, older patients may move across states, creating further matching dilemmas. We are unaware
319 of any alternative algorithm that does better using this data with only these fields available.

320 5 De-duplication

321 Our application of SMERE to the NLTCs assumes that each list had no duplicates, however,
322 many other applications will contain duplicates within lists. We showed in Section 3.1 that we can
323 theoretically handle de-duplication across and within lists. We apply SMERE with de-duplication
324 (SMERED) to the NLTCs by (i) running SMERED on the three waves to show that the algorithm
325 does not falsely detect duplicates when there really are none, and (ii) combining all the lists into
326 one file, hence creating many duplicates, to show that SMERED can find them.

327 5.1 Application to NLTCs

328 We combine the three files of the NLTCs mentioned in Section 4 which contain 22,132 duplicate
329 records out of 57,077 total records. We run SMERED on settings (i) and (ii), evaluating accuracy
330 with the unique IDs.

331 In the case of running SMERED on the three waves, we compare our results of SMERED and
332 SMERE to that under “ground truth” (Table 4). In the case of the NLTCs, compiling all three files
333 together and running the three waves separately under SMERED yields similar results, since we
334 match on similar covariate information. There is no covariate information to add to from thorough
335 investigation to improve our results, except under simulation study.

336 When running SMERE for three files, the FNR is 0.11 and the FPR is 0.37. When running
337 SMERED and estimating a single linkage structure by linking records in shared most probable

maximal matching sets, the FNR is 0.11 and the FPR is 0.37. We contrast this with the results 338
obtained when running SMERED under the shared most probable MMSs (MPMMS) for a single 339
compiled file (Table 5), which yields an FNR of 0.10 and an FPR of 0.17. Clearly, SMERE produces 340
the best results in terms of both FNR and FPR; however, if we want to consider the record linkage 341
and de-duplication problem simultaneously, the SMERED algorithm with linkages applied through 342
the shared MPMMS lowers the FPR nearly in half. 343

The dramatic increase in the FPR and number of false links shown in Table 4 is explained by 344
how few field variables we match on. Their small number means that there are many records for 345
different individuals that have identical or near-identical values. On examination, there are 2,558 346
possible matches among “twins,” records which agree exactly on all attributes but have different 347
unique IDs. Moreover, there are 353,536 “near-twins,” pairs of records that have different unique 348
IDs but match on all but one attribute. This illustrates why the matching problem is so hard 349
for the NLTCs and other data sources like it, where survey-responder information like name and 350
address are lacking. However, if it is known that each file contains no duplicates, there is no need 351
to consider most of these twins and near-twins as possible matches. 352

We would like to put SMERED’s error rates in perspective by comparing to another method, 353
but we know of no other that simultaneously links and de-duplicates three or more files. Thus, we 354
compare to the simple baseline of linking records when, and only when, they agree on all fields (cf. 355
Fleming, King and Juda, 2007). See Table 4 for the relevant error rates. Recall that SMERED 356
produces a FNR and FPR of 0.10 and 0.37. The baseline has an FPR of 0.09, much lower than 357
ours, and an FNR of 0.09, which is the same. We attribute the comparatively good performance 358
of the baseline to there being only five categorical fields per record. With more information per 359
record, exact matches would be much rarer, and the baseline’s FPR would shrink while its FNR 360
would tend to 1. Furthermore, we extend the baseline to the idea of “near-twins.” Under this, we 361
find that the FPR and FNR are 12.61 and 0.05, where the FPR is orders of magnitude larger than 362
ours, while the FNR is slightly lower. While the FPR is high under our model, it is much worse 363
for the baseline of “near-twins.” Our methods tend to “lump” distinct latent individuals, but it is 364
much less prone to lump than the baseline, at a minor cost in splitting. 365

366 We also consider a slightly modified version of our proposed methodology wherein we estimate
367 the overall linkage structure by linking those records that are in any shared MMS with a posterior
368 probability of at least 0.8. The resulting linkage structure is still guaranteed to be transitive, but
369 it includes fewer links. This procedure attains a similar FNR (0.10) to the original methodology,
370 but it has a substantially lower FPR (0.17).

371 Furthermore, we compare to the baseline using a range of thresholded FNRs and FPRs using the
372 shared most probable MMSs. We apply thresholded values ranging from [0.2,1] to the shared most
373 probable MMSs (and after thresholding calculating each FNR and FPR). This allows us to plot
374 the tradeoff for FNR and FPR under under SMERE and SMERED as seen in Figure 5. SMERE
375 and SMERED perform similarly compared to the baseline of exact matching, however, we note
376 that either FPR or FNR can be changed for better performance to be gained. When the baseline
377 changes to “near-twins,” however, both our algorithms in terms of performance radically beat the
378 “near-twins” baseline, showing the value of a model-based approach when there are distortions
379 or noise in the data. We are not able to catch *all* of the effects of distortion; but, under a very
380 simplistic and easily implemented model, where we match on very little information, we do well.

381 6 Discussion

382 We have made two contributions in this paper. The first and more general one is to frame record
383 linkage and de-duplication simultaneously, namely linking observed records to latent individuals
384 and representing the linkage structure via Λ . The second contribution is our specific parametric
385 Bayesian model, which, combined with the linkage structure, allows for efficient inference and
386 exact error rate calculation (such as our most probable MMS and associated posterior probabilities).
387 Moreover, this allows for easy integration with capture-recapture methods, where error propagation
388 is *exact*. As with any parametric model, its assumptions only apply to certain problems; however,
389 this work serves as a starting point for more elaborate models, e.g., incorporating missing fields, data
390 fusion, complicated string fields, population heterogeneity, or dependence across fields, across time,
391 or across individuals. Within the Bayesian paradigm, such model expansions will lead to larger
392 parameter spaces, and therefore call for computational speed-ups, perhaps via online learning,

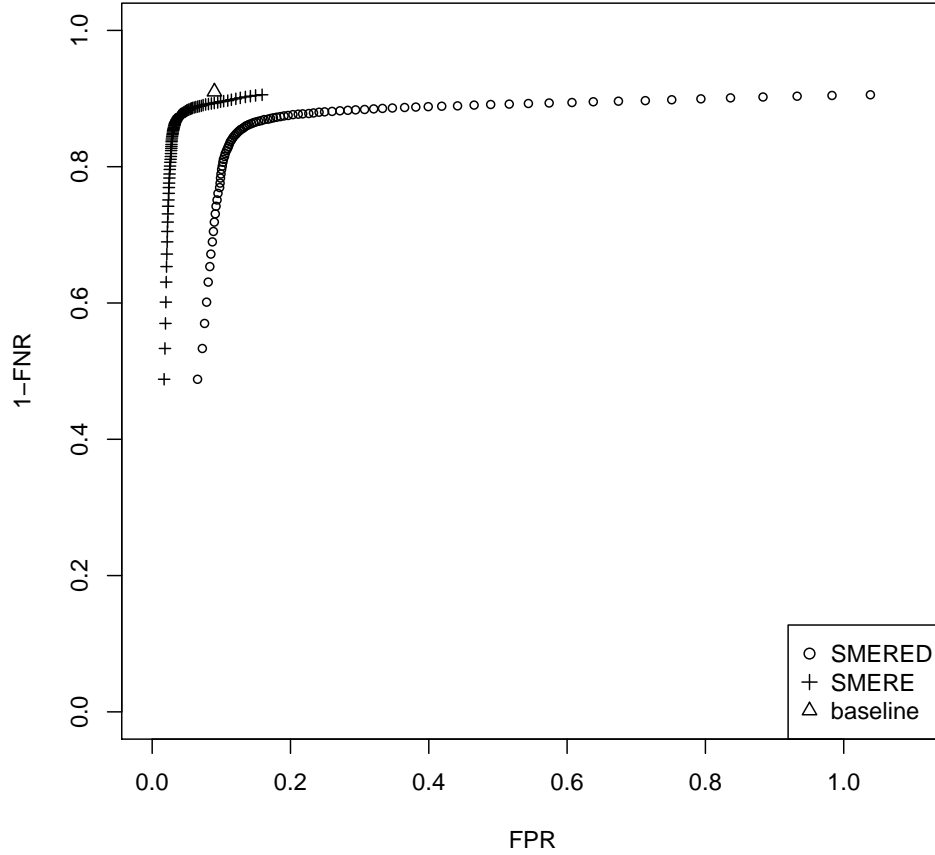


Figure 5: We plot both receiver operating characteristics (ROC) curves under SMERE and SMERED for the most probable MMSs (this is to avoid all to all comparisons) and compare them to the simple baseline (triangle). For the same FNR (\approx the number of missing links), the FPR (\approx the number of false links) is higher under SMERED than under SMERE. This is again due to problems in linkage using SMERED when the categorical information is very limited. When the FNR is small, performance is very similar under SMERE and SMERED. However, we note that the baseline can *never change*, whereas, under our algorithm we can relax the FPR or FNR for performance. The “near-twins” baseline does not appear on this plot since its FPR is 12.61.

393 variational inference, or approximate Bayesian computation.

394 Our work serves as a first basis for solving record linkage and de-duplication problems simula-
395 teously using a noisy Bayesian model and a linkage structure that can handle large-scale databases.
396 We hope that our approach will encourage the emergence of new record linkage approaches and
397 applications along with more state-of-the-art algorithms for this kind of high-dimensional data.

sets of records	1.10084	3.5583; 1.10084	3.5583; 1.10084; 2.6131
posterior probability	0.001	0.004	0.995

Table 3: Example of posterior matching probabilities for record 10084 in 1982

	82	89	94	82, 89	89, 94	82, 94	82, 89, 94
NLTCS (ground truth)	7955	2959	7572	4464	3929	1511	6114
Bayes Estimates _{SMERE}	7964.0	3434.1	8937.8	4116.9	4502.1	1632.2	5413.0
Bayes Estimates _{SMERED}	7394.7	3009.9	6850.4	4247.5	3902.7	1478.7	5191.2
Relative Errors _{SMERE} (%)	0.11	16.06	18.04	-7.78	14.59	8.02	-11.47
Relative Errors _{SMERED} (%)	-7.04	1.72	-9.53	-4.85	-0.67	-2.14	-15.09

Table 4: Comparing NLTCS (ground truth) to the Bayes estimates of matches for SMERE and SMERED

	False links	True Links	Missing Links	FNR	FPR
NLTCS (ground truth)	0	28246	0	0	0
Bayes Estimates _{SMERE}	1299	25196	3050	0.11	0.05
Bayes Estimates _{SMERED}	10595	24900	3346	0.09	0.37
MPMMS _{SMERED}	4819	25489	2757	0.10	0.17
Exact matching	2558	25666	2580	0.09	0.09
Near-twins matching	356094	26936	1310	0.05	12.61

Table 5: False, True, and Missing Links for NLTCS under blocking sex and DOB year where the Bayes estimates are calculated in the absence of duplicates per file and when duplicates are present (when combining all three waves). Also, reported FNR and FPR for NLTCS, Bayes estimates.

398 References

- 399 BELIN, T. R. and RUBIN, D. B. (1995). A method for calibrating false-match rates in record
400 linkage. *Journal of the American Statistical Association*, **90** 694–707.
- 401 CHRISTEN, P. (2011). A survey of indexing techniques for scalable record linkage and deduplication.
402 *IEEE Transactions on Knowledge and Data Engineering*, **99**.
- 403 COPAS, J. and HILTON, F. (1990). Record linkage: Statistical models for matching computer
404 records. *Journal of the Royal Statistical Society, Series A*, **153** 287–320.
- 405 DOMINGOS, P. and DOMINGOS, P. (2004). Multi-relational record linkage. In *Proceedings of the*
406 *KDD-2004 Workshop on Multi-Relational Data Mining*. ACM.
- 407 FELLEGI, I. and SUNTER, A. (1969). A theory for record linkage. *Journal of the American*
408 *Statistical Association*, **64** 1183–1210.
- 409 FLEMING, L., KING, C., III and JUDA, A. (2007). Small worlds and regional innovation. *Organi-*
410 *zation Science*, **18** 938–954.
- 411 GUTMAN, R., AFENDULIS, C. and ZASLAVSKY, A. (2013). A bayesian procedure for file linking to
412 analyze end- of-life medical costs. *Journal of the American Statistical Association*, **108** 34–47.
- 413 HALL, R. and FIENBERG, S. (2012). Valid statistical inference on automatically matched files. In
414 *Privacy in Statistical Databases 2012* (J. Domingo-Ferrer and I. Tinnirello, eds.), vol. 7556 of
415 *Lecture Notes in Computer Science*. Springer, Berlin, 131–142.
- 416 HERZOG, T., SCHEUREN, F. and WINKLER, W. (2007). *Data Quality and Record Linkage Tech-*
417 *niques*. Springer, New York.
- 418 JAIN, S. and NEAL, R. (2004). A split-merge Markov chain Monte Carlo procedure for the Dirichlet
419 process mixture model. *Journal of Computational and Graphical Statistics*, **13** 158–182.
- 420 LAHIRI, P. and LARSEN, M. (2005). Regression analysis with linked data. *Journal of the American*
421 *Statistical Association*, **100** 222–230.

- LARSEN, M. D. and RUBIN, D. B. (2001). Iterative automated record linkage using mixture models. *Journal of the American Statistical Association*, **96** 32–41.
- LISEO, B. and TANCREDI, A. (2013). Some advances on Bayesian record linkage and inference for linked data. URL http://www.ine.es/e/essnetdi_ws2011/ppts/Liseo_Tancredi.pdf.
- REITER, J. P. and RAGHUNATHAN, T. E. (2007). The multiple adaptations of multiple imputation. *Journal of the American Statistical Association*, **102** 1462–1471.
- SADINLE, M. and FIENBERG, S. (2013). A generalized Fellegi-Sunter framework for multiple record linkage with application to homicide record-systems. *Journal of the American Statistical Association*, **108** 385–397.
- TANCREDI, A. and LISEO, B. (2011). A hierarchical Bayesian approach to record linkage and population size problems. *Annals of Applied Statistics*, **5** 1553–1585.
- WINKLER, W. (1999). The state of record linkage and current research problems. Technical report, Statistical Research Division, U.S. Bureau of the Census.
- WINKLER, W. (2000). Machine learning, information retrieval, and record linkage. American Statistical Association, Proceedings of the Section on Survey Research Methods, 20–29. URL <http://www.niss.org/affiliates/dqworkshop/papers/winkler.pdf>.

438 **A Motivating Example of Linkage Structure and Distortion**

We now present a simple example of the ideas of distortion and linkage, which illustrates the relationships between the observed data \mathbf{X} , the latent individuals \mathbf{y} , the linkage structure $\mathbf{\Lambda}$, and the distortion indicators \mathbf{z} . Suppose the “population” (individuals represented in at least one list) has four members, where name and address are stripped for anonymity and they are listed by state, age, and sex. For instance, the latent individual vector \mathbf{y} might be

$$\mathbf{y} = \begin{bmatrix} \text{NC, 72, F} \\ \text{SC, 73, F} \\ \text{PA, 91, M} \\ \text{VA, 94, M} \end{bmatrix}.$$

The observed records \mathbf{X} are given in three separate lists, which would combine into a three-dimensional array. We write this here as three two-dimensional arrays for notational simplicity:

$$\text{List 1} = \begin{bmatrix} \text{NC, 72, F} \\ \text{SC, 70, F} \\ \text{PA, 91, M} \end{bmatrix}, \quad \text{List 2} = \begin{bmatrix} \text{SC, 37, F} \\ \text{VA, 93, M} \\ \text{PA, 92, M} \end{bmatrix}, \quad \text{List 3} = \begin{bmatrix} \text{NC, 72, F} \\ \text{NC, 72, F} \\ \text{SC, 72, F} \\ \text{VA, 94, M} \end{bmatrix}$$

439 Here, for the sake of keeping the illustration simple, only age is distorted.

440 Comparing \mathbf{X} to \mathbf{y} , the intended linkage and distortions are then

$$\mathbf{\Lambda} = \begin{bmatrix} 1 & 2 & 3 \\ 2 & 4 & 3 \\ 1 & 1 & 2 & 4 \end{bmatrix}, \quad \mathbf{z}_1 = \begin{bmatrix} 0 & 0 & 0 \\ 0 & 1 & 0 \\ 0 & 0 & 0 \end{bmatrix}, \quad \mathbf{z}_2 = \begin{bmatrix} 0 & 1 & 0 \\ 0 & 1 & 0 \\ 0 & 1 & 0 \end{bmatrix}, \quad \mathbf{z}_3 = \begin{bmatrix} 0 & 0 & 0 \\ 0 & 0 & 0 \\ 0 & 1 & 0 \\ 0 & 0 & 0 \end{bmatrix}.$$

441 In this linkage structure, every entry of $\mathbf{\Lambda}$ with a value of 2 means that some record from \mathbf{X} refers
 442 to the latent individual with attributes “SC, 73, F.” Here, the age of this individual is distorted in

all three lists, as can be seen from \mathbf{z} . (Note that \mathbf{z} , like \mathbf{X} , is also really a three-dimensional array.) 443
 Looking at \mathbf{z}_1 and \mathbf{z}_3 , we see that there is only a single record in either list that is distorted, and it 444
 is only distorted in one field. In list 2, however, every record is distorted, though only in one field. 445

Figure 6 illustrates the interpretation of our linkage structure as a bipartite graph in which each 446
 edge links a record to a latent individual. For clarity, Figure 6 shows that X_{11} and X_{22} are the 447
 same individual and shows that X_{13} , X_{21} , and X_{34} correspond to the same individual. The rest are 448
 non-matches. 449

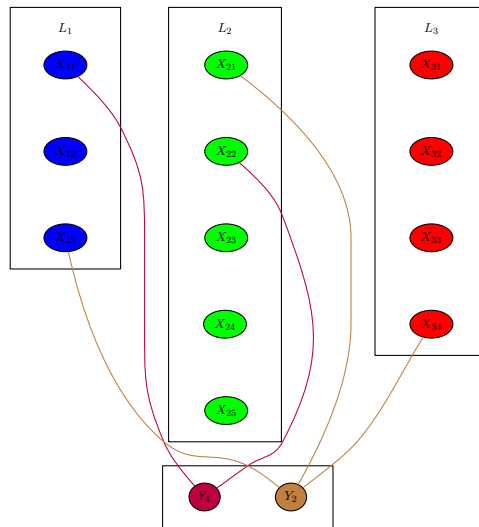


Figure 6: Illustration of records \mathbf{X} , latent random variables \mathbf{Y} , and linkage (by edges) $\mathbf{\Lambda}$.

B Hybrid MCMC Algorithm (SMERED) 450

We now describe in more detail the Metropolis-within-Gibbs algorithm with split-merge proposals 451
 and optional record linkage blocking (with pseudo-code given at the end). The entire loop below 452
 is repeated for a number of MCMC iterations $S_H = S_G \times S_M$. Additionally, the algorithm allows 453
 multiple split-merge operations to be performed in a single Metropolis-Hastings proposal step. Let 454
 T denote the allowed number of split-merge operations within each Metropolis-Hastings step. Let 455
 $\mathbf{\Lambda}^{(m)}, \mathbf{y}^{(m)}, \mathbf{z}^{(m)}, \boldsymbol{\theta}^{(m)}, \boldsymbol{\beta}^{(m)}$ denote the values of the MCMC chain at step m . 456

1. Repeat the following sequence of steps T times: 457

- 458 (a) As already described in Section 3.2, we sample pairs of records from different files uni-
459 formly at random within blocks.
- 460 (b) If the two records chosen above in (a) are currently assigned to the same latent individual,
461 we propose to split them as follows:
- 462 i. Let j' denote the latent individual to which both records are currently assigned.
 - 463 ii. Let C denote the set of all *other* records—not including the two chosen in step (a)
464 above—who are also assigned to latent individual j' . Note that this set C may be
465 empty.
 - 466 iii. Give the two records new assignments of latent individuals, calling these new as-
467 signments j_1 and j_2 . One of the two individuals stays assigned to j' , while the other
468 is assigned to a latent individual currently not assigned to any records.
 - 469 iv. Randomly assign all the other records in C to either j_1 or j_2 , which partitions
470 C into sets C_1 and C_2 . The inclusion of this step is important as the algorithm
471 does not actually actually split or merge *records*—it actually splits or merges *latent*
472 *individuals*. Note that the sets C_1 and C_2 are designed to *include* the two records
473 we chose in step (a).
 - 474 v. The latent individuals j_1 and j_2 get their values \mathbf{y}'_{j_1} and \mathbf{y}'_{j_2} assigned by simply
475 taking them to be *equal* (without distortion) to the exact record values for one of
476 the individuals in the sets C_1 and C_2 (respectively), chosen at random.
 - 477 vi. For each record in C_1 and C_2 , the corresponding distortion indicators $z'_{ij\ell}$ for each
478 field are resampled from their respective conditional distributions. Note that some
479 of these may be guaranteed to automatically be 1 (whenever a record differs from
480 its corresponding latent individual on a particular field).
 - 481 vii. The above steps generate new proposals $\mathbf{\Lambda}'$, \mathbf{y}' , and \mathbf{z}' . We now decide whether to
482 accept or reject the proposal according to the Metropolis acceptance probability. If
483 we accept the proposal, then we take $\mathbf{\Lambda}^{(m+1)} = \mathbf{\Lambda}'$, $\mathbf{y}^{(m+1)} = \mathbf{y}'$, and $\mathbf{z}^{(m+1)} = \mathbf{z}'$. If
484 we reject the proposal, then we take $\mathbf{\Lambda}^{(m+1)} = \mathbf{\Lambda}^{(m)}$, $\mathbf{y}^{(m+1)} = \mathbf{y}^{(m)}$, and $\mathbf{z}^{(m+1)} =$
485 $\mathbf{z}^{(m)}$.

Algorithm 1: Split and MErgE REcord linkage and Deduplication (SMERED)

Data: \mathbf{X} and hyperparameters

Initialize the unknown parameters $\boldsymbol{\theta}, \boldsymbol{\beta}, \mathbf{y}, \mathbf{z}$, and $\boldsymbol{\Lambda}$.

```

for  $i \leftarrow 1$  to  $S_G$  do
  for  $j \leftarrow 1$  to  $S_M$  do
    for  $t \leftarrow 1$  to  $S_T$  do
      Draw records  $R_1$  and  $R_2$  uniformly and independently at random.
      if  $R_1$  and  $R_2$  refer to the same individual then
        propose splitting that individual, shifting  $\boldsymbol{\Lambda}$  to  $\boldsymbol{\Lambda}'$ 
         $r \leftarrow \min \{1, \pi(\boldsymbol{\Lambda}', \mathbf{y}, \mathbf{z}, \boldsymbol{\theta}, \boldsymbol{\beta} | \mathbf{x}) / \pi(\boldsymbol{\Lambda}, \mathbf{y}, \mathbf{z}, \boldsymbol{\theta}, \boldsymbol{\beta} | \mathbf{x})\}$ 
      endif
      else
        propose merging the individuals  $R_1$  and  $R_2$  refer to, shifting  $\boldsymbol{\Lambda}$  to  $\boldsymbol{\Lambda}'$ 
         $r \leftarrow \min \{1, \pi(\boldsymbol{\Lambda}', \mathbf{y}, \mathbf{z}, \boldsymbol{\theta}, \boldsymbol{\beta} | \mathbf{x}) / \pi(\boldsymbol{\Lambda}, \mathbf{y}, \mathbf{z}, \boldsymbol{\theta}, \boldsymbol{\beta} | \mathbf{x})\}$ 
      endif
      Resampling  $\boldsymbol{\Lambda}$  by accepting proposal with Metropolis probability  $r$  or rejecting
      with probability  $1 - r$ .
    end
    Resample  $\mathbf{y}$  and  $\mathbf{z}$ .
  end
  Resample  $\boldsymbol{\theta}, \boldsymbol{\beta}$ .
end
return  $\boldsymbol{\theta} | \mathbf{X}, \boldsymbol{\beta} | \mathbf{X}, \mathbf{y} | \mathbf{X}, \mathbf{z} | \mathbf{X}$ , and  $\boldsymbol{\Lambda} | \mathbf{X}$ .
  
```

(c) If instead the two records chosen above in (a) are currently assigned to different latent 486
 individuals, we propose to merge them. The same basic steps happen: a new state 487
 is created in which all records which belong to the same individual as either input 488
 record are all merged into a new individual. The fields for this individual are sampled 489
 uniformly from these records, distortion variables are all re-sampled, and then acceptance 490
 probability is tested. 491

2. Finally, new values $\boldsymbol{\theta}^{(m+1)}$ and $\boldsymbol{\beta}^{(m+1)}$ are drawn from their distributions conditional on the values of $\boldsymbol{\Lambda}^{(m+1)}$, $\mathbf{y}^{(m+1)}$, and $\mathbf{z}^{(m+1)}$ that we just selected:

$$\boldsymbol{\theta}^{(m+1)}, \boldsymbol{\beta}^{(m+1)} \stackrel{\text{draw}}{\sim} \pi(\boldsymbol{\theta}, \boldsymbol{\beta} | \mathbf{y}^{(m)}, \mathbf{z}^{(m)}, \boldsymbol{\Lambda}^{(m)}, \mathbf{x}).$$

492 **B.1 Time Complexity**

493 Scalability is crucial to any record linkage algorithm. Current approaches typically run in poly-
 494 mial (but super-linear) time in N_{\max} . (The method of [Sadinle and Fienberg \(2013\)](#) is $O(N_{\max}^k)$,
 495 while that of [Domingos and Domingos \(2004\)](#) finds the maximum flow in an N_{\max} -node graph,
 496 which is $O(N_{\max}^3)$, but independent of k .) In contrast, our algorithm is linear in both N_{\max} and
 497 MCMC iterations.

498 Our running time is proportional to the number of Gibbs iterations S_G , so we focus on the time
 499 taken by one Gibbs step. Recall the notation from Section 3, and define $M = \frac{1}{p} \sum_{\ell=1}^p M_{\ell}$ as the
 500 average number of possible values per field ($M \geq 1$). The time taken by a Gibbs step is dominated
 501 by sampling from the conditional distributions. Specifically, sampling β and y are both $O(pN_{\max})$;
 502 sampling θ is $O(pMN) + O(pN_{\max}) = O(pMN)$, as is sampling z . Sampling \mathbf{A} is $O(pN_{\max}M)$ if
 503 done carefully. Thus, all these samples can be drawn in time linear in N_{\max} .

504 Since there are S_M Metropolis steps within each Gibbs step and each Metropolis step updates y ,
 505 z , and \mathbf{A} , the time needed for the Metropolis part of one Gibbs step is $O(S_M p N_{\max}) + O(S_M p MN) +$
 506 $O(S_M p N_{\max} M)$. Since $N \leq N_{\max}$, the run time becomes $O(p S_M N_{\max}) + O(M p S_M N_{\max}) =$
 507 $O(M p S_M N_{\max})$. On the other hand, the updates for θ and β occur once each Gibbs step im-
 508 plying the run time is $O(pMN) + O(pN_{\max})$. Since $N \leq N_{\max}$, the run time becomes $O(pMN_{\max} +$
 509 $pN_{\max}) = O(pMN_{\max})$. The overall run time of a Gibbs step is $O(pMN_{\max} S_M) + O(pMN_{\max}) =$
 510 $O(pMN_{\max} S_M)$. Furthermore, for S_G iterations of the Gibbs sampler, the algorithm is order
 511 $O(pMN_{\max} S_G S_M)$. If p and M are all much less than N_{\max} , we find that the run time is $O(N_{\max} S_G S_M)$.

512 Another important consideration is the number of MCMC steps needed to produce Gibbs sam-
 513 ples that form an adequate approximation of the true posterior. This issue depends on the conver-
 514 gence properties of the hybrid Markov chain used by the algorithm, which are beyond the scope of
 515 the present work.

C Simulation Study

516

We provide a simulation study based on the model in Section 3.1, and we simulate data from the NLTCS based on our model, with varying levels of distortion. The varying levels of distortion (0, 0.25%, 0.5%, 1%, 2%, 5%) associated with the simulated data are then run using our MCMC algorithm to assess how well we can match under “noisy data.” Figure 7 illustrates an approximate linear relationship with FPR (plusses) and the distortion level, while for FNR (triangles) exhibits a sudden large increase as the distortion level moves from 2% to 5%. Figure 8 demonstrates that for moderate distortion levels (per field), we can estimate the true number of observed individuals extremely well via estimated posterior densities. However, once the distortion is too *noisy*, our model has trouble recovering this value.

517

518

519

520

521

522

523

524

525

In summary, as records become more noisy or distorted, our matching algorithm typically matches less than 80% of the individuals. Furthermore, once the distortion is around 5%, we can only hope to recover approximately 65% of the individuals. Nevertheless, this degree of accuracy is in fact quite encouraging given the noise inherent in the data and given the relative lack of identifying variables on which to base the matching.

526

527

528

529

530

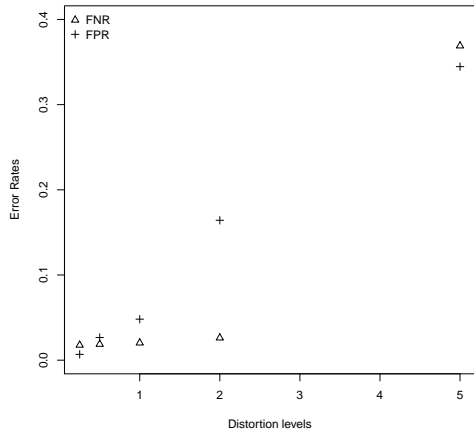


Figure 7: FNR and FPR versus distortion percentage. FPR shows an approximately linear relationship with distortion percentage, while FNR exhibits a sudden large increase as the distortion level moves from 2% to 5%.

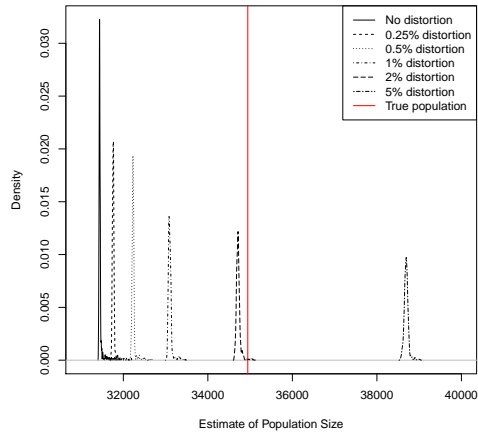


Figure 8: Posterior density estimates for 6 levels of distortion (none, 0.25%, 0.5%, 1%, 2%, and 5%) compared to ground truth (in red). As distortion increases (and approaches 2% per field), we overmatch N , however as distortion quickly increases to high levels (5% per field), the model undermatches. This behavior is expected to increase for higher levels of distortion. The simulated data illustrates that under our model, we are able to capture the idea of moderate distortion (per field) extremely well.

D Confusion Matrix for NLTCS

531

Est vs Truth	82	89	82,89	94	82, 94	89, 94	AY	RS
82	8051.9	0.0	385.1	0.0	162.9	0.0	338.6	8938.5
89	0.0	2768.4	291.1	0.0	0.0	240.6	131.7	341.8
82, 89	118.4	2.2	8071.7	0.0	4.4	0.4	803.2	9000.3
94	0.0	0.0	0.0	7255.4	139.3	240.5	325.12	7960.32
82, 94	163.1	0.0	9.5	97.0	2662.2	0.09	331.5	3263.39
89, 94	0.0	186.8	6.1	190.6	1.5	7365.8	488.2	8239
AY	62.5	1.6	164.4	28.9	51.7	10.6	15923.7	18342.02
NLTCS	8396	2959	4464	7572	1511	3929	6114	

Table 6: Confusion Matrix for NLTCS

Est vs Truth	82	89	82,89	94	82, 94	89, 94	AY
82	0.9600	0.00000	0.04300	0.0000	0.0540	0.0000	0.0180
89	0.0000	0.94000	0.03300	0.0000	0.0000	3.1e-02	0.0072
82, 89	0.0140	0.00074	0.90000	0.0000	0.0015	5.1e-05	0.0440
94	0.0000	0.00000	0.00000	0.9600	0.0460	3.1e-02	0.0180
82,94	0.0190	0.00000	0.00110	0.0130	0.8800	1.1e-05	0.0180
89,94	0.0000	0.06300	0.00068	0.0250	0.0005	9.4e-01	0.0270
AY	0.0074	0.00054	0.01800	0.0038	0.0170	1.3e-03	0.8700

Table 7: Misclassification errors of confusion matrix for NLTCS